2012

Riverine source of Arctic Ocean mercury inferred from atmospheric observations

Jenny A. Fisher
Harvard University, jennyf@uow.edu.au

Daniel J. Jacob
Harvard University

Anne L. Soerensen
Harvard University

Helen M. Amos
Harvard University

Alexandra Steffen
Environment Canada

See next page for additional authors

Riverine source of Arctic Ocean mercury inferred from atmospheric observations

Abstract

Methylmercury is a potent neurotoxin that accumulates in aquatic food webs. Human activities, including industry and mining, have increased inorganic mercury inputs to terrestrial and aquatic ecosystems. Methylation of this mercury generates methylmercury, and is thus a public health concern. Marine methylmercury is a particular concern in the Arctic, where indigenous peoples rely heavily on marine-based diets. In the summer, atmospheric inorganic mercury concentrations peak in the Arctic, whereas they reach a minimum in the northern mid-latitudes. Here, we use a global three-dimensional ocean–atmosphere model to examine the cause of this Arctic summertime maximum. According to our simulations, circumpolar rivers deliver large quantities of mercury to the Arctic Ocean during summer; the subsequent evasion of this riverine mercury to the atmosphere can explain the summertime peak in atmospheric mercury levels. We infer that rivers are the dominant source of mercury to the Arctic Ocean on an annual basis. Our simulations suggest that Arctic Ocean mercury concentrations could be highly sensitive to climate-induced changes in river flow, and to increases in the mobility of mercury in soils, for example as a result of permafrost thaw and forest fires.

Keywords

riverine, observations, atmospheric, arctic, inferred, source, mercury, ocean, GeoQUEST

Disciplines

Life Sciences | Physical Sciences and Mathematics | Social and Behavioral Sciences

Publication Details

Fisher, J. A., Jacob, D. J., Soerensen, A. L., Amos, H. M., Steffen, A. & Sunderland, E. M. (2012). Riverine source of Arctic Ocean mercury inferred from atmospheric observations. Nature Geoscience, 5 (7), 499-504.

Authors

Jenny A. Fisher, Daniel J. Jacob, Anne L. Soerensen, Helen M. Amos, Alexandra Steffen, and Elsie M. Sunderland

This article was originally published as :
Fisher, J. A., Jacob, D. J., Soerensen, A. L., Amos, H. M., Steffen, A. & Sunderland, E. M. (2012). Riverine source of Arctic Ocean mercury inferred from atmospheric observations. *Nature Geoscience*, 5 (7), 499-504.

Major riverine source of Arctic Ocean mercury inferred from atmospheric observations

Jenny A. Fisher[1*], Daniel J. Jacob[1,2], Anne L. Soerensen[2,3], Helen M. Amos[1], Alexandra Steffen[4], and Elsie M. Sunderland[2,3]

[1]Department of Earth and Planetary Sciences, Harvard University, Cambridge, Massachusetts 02138, USA

[2]School of Engineering and Applied Sciences, Harvard University, Cambridge, Massachusetts 02138, USA

[3]Department of Environmental Health, Harvard School of Public Health, Harvard University, Boston, Massachusetts 02215, USA

[4]Air Quality Processes Research Section, Environment Canada, Toronto, Ontario M3H 5T4, Canada

*e-mail: jafisher@fas.harvard.edu

Methylmercury is a potent neurotoxin that bioaccumulates in aquatic food-webs. Human activities including industry and mining have increased the loading of inorganic mercury to terrestrial and aquatic ecosystems, and methylation of this mercury has become a public health concern. Elevated mercury in the Arctic Ocean is of particular concern as indigenous populations rely heavily on marine-based diets. Here we use a three-dimensional ocean-atmosphere model (GEOS-Chem) to interpret the observed seasonal variation of atmospheric mercury in the Arctic. We argue that the observed summer maximum cannot be explained by atmospheric transport, emission from snow, or ocean kinetics. Instead, we propose that it is driven by evasion from the Arctic Ocean, where concentrations have been enriched by a large seasonal mercury source from circumpolar rivers. We infer that rivers may be the dominant source of mercury to the Arctic Ocean on an annual basis. This finding implies a strong sensitivity of Arctic mercury to climate change through increasing river flow and increasing soil mobility of mercury (thawing permafrost, forest fires).

Mercury is emitted from anthropogenic and natural sources primarily as elemental mercury (Hg^0). The Hg^0 atmospheric lifetime of 6-12 months allows transport of this emitted mercury on a hemispheric scale. Eventual oxidation to highly soluble Hg^{II} drives deposition in remote regions. Hg^0 has been measured continuously at sites across the Arctic since the mid-1990s[1-3]. As seen in Fig. 1, Hg^0 concentrations in surface air at high Arctic coastal sites display a strong seasonality with minimum in spring and maximum in summer. This contrasts with observations at northern mid-latitudes that show a weak minimum in late summer due to destruction by photochemically-produced oxidants[4]. The spring decrease in the Arctic reflects Atmospheric

Mercury Depletion Events (AMDEs) initiated by the photochemical release of bromine radicals ($BrO_x \equiv Br+BrO$) from sea salt concentrated in sea ice[5]. High BrO_x concentrations drive rapid oxidation of Hg^0 to Hg^{II} (ref. 6) and subsequent deposition to snow and ice.

The summer maximum of Hg^0 in the Arctic atmosphere is less understood. It was initially attributed to re-emission of mercury deposited to snow and ice during spring[7]. Recent work has called this assumption into question[1], invoking instead an oceanic source[3,8,9]. Atmosphere-ocean Hg^0 exchange is expected to display strong seasonality driven by variations in sea-ice cover, temperature, freshwater inputs, and light availability. Arctic Ocean cruise data show elevated summertime concentrations of mercury both above and below sea ice[10-12], suggesting large fluxes of Hg^0 to the atmosphere from supersaturated ocean waters[12]. However, the mechanisms supplying the oceanic pool of Hg^0 subject to evasion have not been explained.

Seasonal variation of Arctic mercury

Figure 1 shows the mean observed seasonal cycle of atmospheric Hg^0 at three high Arctic sites: Alert (Canada), Amderma (Russia), and Zeppelin Mountain (Ny Ålesund, Norway). Concentrations vary in amplitude across the three sites but all show similar seasonality, with minimum in April-May and maximum in July. Fall-winter concentrations at Arctic sites show no mean significant difference from northern mid-latitudes, reflecting the long mercury lifetime relative to the time scales for extratropical mixing.

We simulate the seasonal cycle of atmospheric mercury in the Arctic using the GEOS-Chem global mercury model, which includes a 3-D atmospheric transport and chemistry simulation[13]

dynamically coupled to a 2-D ocean mixed layer simulation with redox chemistry and exchange with subsurface waters[14]. GEOS-Chem has been extensively evaluated with atmospheric and oceanic observations[13,14] and has been intercompared with other global and regional mercury models[15,16]. Relative to previous versions[13,14], the present implementation includes a new temperature-dependent scheme for bromine release from sea ice, an improved radiation-dependent treatment of mercury deposited to snow, and updated Arctic-specific ocean parameters for vertical exchange (see Methods). The model does not include lateral transport in the surface ocean, limiting its ability to simulate horizontal gradients across the Arctic Ocean. We focus therefore on simulating the mean seasonal behavior across the three Arctic sites.

Figure 2 compares the multi-year mean observed Hg^0 seasonal variation (black) with that simulated for 2008 by the standard GEOS-Chem model described above (red) and by including changes to various model parameters ("sensitivity simulations"). Simulated seasonality is insensitive to the choice of model year. The standard simulation accurately reproduces the spring decrease driven by AMDEs, which account for 60% of modeled deposition to the Arctic in spring. This largely reflects the assumed dependences of BrO on temperature and of snowpack re-emission on solar radiation (see Methods). 50% of the mercury deposited in AMDEs is re-emitted to the atmosphere in the model, but the net sink is enough to drive a 20% decrease in Hg^0 over the Arctic in spring, consistent with observations (Fig. 2).

We see from Fig. 2 that the standard simulation fails to reproduce the observed summer maximum. It shows only a weak peak in June driven by re-emission from snow, followed by a July-September decrease due to uptake by the ocean. The summer underestimate cannot be

explained by a missing atmospheric source from mid-latitudes since observed summer mercury concentrations shown in Fig. 1 are much higher in the Arctic than at mid-latitudes. The Arctic must therefore be a net atmospheric exporter of mercury rather than importer in summer. This is consistent with statistical analysis of observations at Zeppelin showing that high concentrations are associated with transport from mid-latitudes in winter and spring but not in summer[8]. Atmospheric redox chemistry is also unable to explain the model underestimate in summer as Hg^{II} accounts for <2% of total Arctic gas-phase mercury both in the model and in observations[11,17].

We investigated whether the summer peak could be driven by re-emission of mercury deposited to the Arctic cryosphere in spring. Observational constraints on in-snow reduction and re-emission of deposited mercury show large uncertainties[18]. We performed sensitivity simulations for both continental and sea-ice snow with (1) the reducible percentage of mercury in snow increased from 60% in the standard model[13] to 90% (an upper limit from observations[19]) and (2) the net in-snow reduction rate constant increased by a factor of 100 (consistent with the spread of observational estimates[18], see Methods). Results shown in Fig. 2 (purple) indicate negligible impact on either the timing or the magnitude of the summer peak. This is because re-emission can only take place in a narrow seasonal window between the onset of radiation (April) and the onset of snowmelt (May-June), when dissolved mercury is rapidly eluted from the snowpack during an ionic pulse lasting only a few days[18]. When the snowpack reduction rate is increased, the snowpack becomes depleted earlier and atmospheric concentrations in June are actually lower than in the standard simulation. When the snowpack reduction rate is decreased, the snow mercury reservoir is removed with the meltwater before re-emission can occur.

Mercury added to the ocean mixed layer may be re-emitted to the atmosphere by reduction of dissolved Hg^{II} to Hg^0 or transferred to the subsurface ocean by wind-driven mixing and particle settling. Figure 3a shows the modeled seasonal budget of total mercury (THg ≡ Hg^0 + Hg^{II}; see Methods) in the ocean mixed layer, with inputs (meltwater, entrainment from subsurface waters, and atmospheric deposition) in red and outputs (evasion, detrainment to subsurface waters, and particle settling) in blue. Removal from the mixed layer to subsurface waters peaks during spring and summer, when stratification drives shoaling of the mixed layer[20,21] and increased biological productivity enhances losses associated with settling particles[22]. These losses to the subsurface ocean exceed atmospheric inputs from direct deposition and meltwater delivery, both in the standard simulation and in a sensitivity simulation with the particle settling flux substantially reduced (see Supplementary Information). The modeled summer minimum in Arctic Ocean mixed layer THg is 1.1 pM, much lower than the 2.8 pM mean of August-October observations from surface waters of the Canadian Arctic[23].

The modeled reservoir of THg in the surface ocean is too small for large evasion fluxes in summer to be driven solely by enhanced reduction of Hg^{II} to Hg^0. Model sensitivity studies confirm that despite observed Hg^0 supersaturation of up to 1800% below sea ice[12], the reducible pool of Hg^{II} (and associated evasion) is rapidly depleted without additional external inputs. We performed a sensitivity simulation (3) increasing the rate of photo-reduction (generally the main pathway for Hg^{II} reduction in the ocean mixed layer[14]) and decreasing the rate of photo-oxidation in the Arctic Ocean both by a factor of five, representing an extreme perturbation. Figure 2

(orange dashed line) shows that the model still cannot sustain a summer maximum even under such unlikely photo-redox conditions.

In coastal Arctic environments, biologically-mediated reduction by mercury-resistant microbes can be a dominant source of Hg^0 even at cold temperatures[24]. Because this reduction pathway is independent of light availability, it can operate in winter and below sea ice and has therefore been suggested as a major driver of dissolved Hg^0 formation across the Arctic[10,24]. We tested this hypothesis with a sensitivity study (4) setting the biotic reduction rate constant to an aseasonal maximum observed value of 2.8×10^{-5} s^{-1} (ref. [25]), about 100 times larger than the global mean value in GEOS-Chem[14]. Results in Fig. 2 (orange dotted line) show that this simulation overestimates atmospheric Hg^0 in winter, which may reflect the assumed aseasonality, but more importantly it still fails to sustain the observed summer maximum.

A potential source from circumpolar rivers

We conclude from the above sensitivity studies that the model must be missing a large seasonal source of mercury to the Arctic Ocean mixed layer in spring-summer and propose that large circumpolar rivers could provide much of that missing source. Rivers are regionally important sources of mercury to other ocean regions, including the Mediterranean Sea and the northern mid-latitude Atlantic[22]. Three of the ten largest rivers in the world are located in the Eurasian Arctic, drawing from large drainage basins and discharging into the small and shallow Arctic Ocean[26]. The flow from circumpolar rivers to the Arctic Ocean accounts for 11% of freshwater inputs to all oceans of the world[27]. These rivers provide a major source of organic carbon to the Arctic Ocean[27] and may also be an important source of mercury as boreal soils and peatlands in

catchment basins are highly enriched in stored mercury[28]. Gold, silver, and mercury mines in Siberia (http://minerals.usgs.gov/minerals/pubs/country/maps/94349.gif) may also provide a large local source of mercury to Russian Arctic rivers.

As shown in Fig. 4, the seasonal cycle of Arctic freshwater discharge from rivers strongly peaks in early summer following ice break-up. In the Mackenzie River, concentrations of both dissolved and particulate mercury are up to 7 times larger during peak flow than later in the year, reflecting increased mercury mobility in drainage-basin soils[29]. As a result, riverine mercury fluxes (the product of mercury concentration and water discharge volume) are up to an order of magnitude larger in early summer than during the rest of the year. The freshwater discharged by rivers remains at the surface of the stratified Arctic Ocean. Combined, these factors suggest that rivers could provide a large seasonal source of Arctic Ocean mercury.

Previous estimates of the annual riverine mercury flux to the Arctic Ocean range from 5-39 Mg a^{-1} but are based on very limited data[30,31]. In each of the three largest Arctic rivers, all in Russia (Yenisei, Lena, and Ob), mercury concentrations have been measured only once, all in the early 1990s and all in September[30], several months after expected peak concentrations. Climate change since that time has increased freshwater discharge[32] and mercury mobilization (permafrost thaw, biogeochemical activity in soil), with expected impacts for riverine mercury concentrations[33]. The limited sampling of Arctic rivers leads to very large uncertainties in the estimated mercury fluxes, even for the better-studied North American rivers. Observations rarely capture the episodic, high-intensity storm events resulting in most mercury discharge, and inferring annual

fluxes from such discrete sampling data leads to significant flux underestimates[34] (see Supplementary Information).

A smaller contribution to the missing source may come from coastal erosion, particularly along the northeast Siberian coast. Erosion takes place mainly in summer, when storm-driven waves in open water can act on coastal sediments[35], but is not expected to peak until early fall when storms are most intense[36]. Because of this seasonal offset, erosion alone cannot replenish the ocean mercury lost to the subsurface in spring. Estimating an annual flux from coastal erosion is challenging as there are no comprehensive data on mercury concentrations in coastal sediments (observations are limited to a single set of cores from the Beaufort coast[37]). Instead, we estimate the erosion contribution based on the better-constrained organic carbon budget. Coastal erosion accounts for up to 15% of the total annual organic carbon flux to the Arctic Ocean, with the rest coming from rivers[38].

To test the importance of these terrigenous sources in the model, we conducted a sensitivity simulation (5) that included an additional source of Hg^{II} to the Arctic Ocean with expected riverine seasonality as shown in Fig. 3b (water flow seasonality of Fig. 4 compounded by riverine mercury concentrations three times higher in May-June than in the rest of the year[39]). The source from coastal erosion would likely be shifted later in the summer and we discuss the implications below. Because the model does not include lateral transport in the ocean, the mercury source is applied uniformly across the Arctic Ocean. The sensitivity to this assumption is discussed in the Supplementary Information. This mercury is then available for evasion from

the ocean mixed layer in areas without continuous sea ice cover (see Supplementary Information) and subsequent atmospheric transport.

We find from this sensitivity simulation that an annual flux of 95 Mg a^{-1} Hg^{II} to the open ocean can provide sufficient mercury to the ocean mixed layer to counteract losses to the subsurface (Fig. 3b), thereby sustaining the summer maximum in ocean evasion apparent in the atmospheric observations (blue line in Fig. 2). The model still shows a peak in June rather than July but this could reflect a delay in mercury transport from the river mouths to offshore waters as well as an offset in the timing of coastal erosion fluxes. Our estimated flux is inferred from the atmospheric observations and reflects the total mercury input to the open ocean needed to drive evasion.

Assuming that the partitioning between rivers and coastal erosion is the same for mercury as for organic carbon (85:15)[38], our total terrigenous flux of 95 Mg a^{-1} might be partitioned into 80 Mg a^{-1} from rivers and 15 Mg a^{-1} from coastal erosion. Translating these fluxes to concentrations is non-trivial due to the uncertain seasonality of the coastal erosion contribution, but we can estimate an upper limit for rivers by assuming they account for the entire flux in early summer, leading to a maximum unfiltered riverine [THg] = 48 ng L^{-1} in June. Limited measurements in Russian rivers showed much lower concentrations, but these samples are not representative of the episodic flood events that drive most riverine transport, as discussed in the Supplementary Information. For coastal erosion, assuming a total annual sediment flux of 430 Mt a^{-1} (ref. 38), our estimated sediment concentration of [THg] = 32 ng g^{-1} is within the range measured along the Beaufort coast (26-303 ng g^{-1})[37].

Our hypothesis of a dominant riverine source to explain the summer mercury maximum in the Arctic atmosphere is consistent with Lagrangian model analyses for Zeppelin by Hirdman et al. [8] showing that the highest summer atmospheric concentrations are associated with an Arctic Ocean source. Closer examination of their source attribution maps shows hotspots in the outflow basins of the Ob, Yenisei, and Kolyma rivers. We conducted additional back trajectory analyses with the NOAA HYSPLIT model (https://ready.arl.noaa.gov/HYSPLIT.php) and find frequent summertime transport to Alert from the central Arctic Ocean and the Eurasian shelf regions as well as transport to Amderma from the outflow regions of the nearby Russian rivers. Inclusion of the riverine source also improves model agreement with mercury measurements in the Arctic Ocean. Mean simulated summer $[Hg^0]$ = 0.21 pM and [THg] = 2.5 pM compare well to July-September observations from across the Arctic Ocean with mean $[Hg^0] = 0.22 \pm 0.11$ pM[12] and to August-October observations from the Canadian Arctic Archipelago with $[Hg^0] = 0.13 \pm 0.06$ pM and [THg] = 2.8 ± 3.1 pM[23]. Further comparisons to observations are shown in Table 1.

Implied budget of Arctic mercury

Figure 5 shows the annual GEOS-Chem model budget of mercury in the Arctic surface ocean-atmosphere-cryosphere system (70-90°N), including a source of 95 Mg a^{-1} from Arctic rivers and coastal erosion. This source dominates the input of mercury to the Arctic surface ocean. In comparison, atmospheric deposition contributes 25 Mg a^{-1} directly to the open ocean and 20 Mg a^{-1} by meltwater runoff following deposition to snow on sea ice. Net annual Hg^0 evasion from the ocean to the atmosphere is 90 Mg a^{-1}. On an annual basis, entrainment and detrainment fluxes between the surface and subsurface waters are roughly balanced, and net transport to the subsurface is mainly by particle settling. There are however large seasonal fluxes driven by

entrainment/detrainment as seen in Fig. 3b. Modeled annual mean mercury concentrations in the Arctic Ocean mixed layer are [THg] = 2.7 pM and [Hg^0] = 0.15 pM, consistent with the limited observations discussed above. More data are thus urgently needed to better quantify the riverine source of mercury to the Arctic Ocean and resolve the many uncertainties in the mercury budget.

The rapid climate change presently taking place in the Arctic is likely altering the riverine mercury source to the Arctic Ocean through changes in watershed dynamics (surface hydrology, mercury mobility, soil biogeochemistry). Mercury stored in boreal soils is becoming increasingly mobilized by thawing permafrost[40] and boreal wildfires[41], and rates of river discharge are increasing[32]. In a follow-up study we will examine how changes in river flow, sea ice cover, and other climate parameters may have affected mercury trends in the Arctic over the past 30 years.

Methods

Model description. We use the GEOS-Chem v9-01-01 mercury simulation (http://geos-chem.org). The simulation is driven by MERRA assimilated meteorological data from the Global Modeling and Assimilation Office (GMAO) Goddard Earth Observing System (GEOS), produced at 0.5°x0.667° horizontal resolution but downgraded here to 4°x5° for input to GEOS-Chem. The MERRA data have 3-hour temporal resolution for atmospheric variables and 1-hour resolution for surface variables (including boundary layer height, surface temperature, and sea ice coverage). Fractional sea ice coverage in MERRA is based on the climatology of Reynolds et al.[42]. The GEOS-Chem atmospheric mercury simulation is described in detail by Holmes et al.[13]. The simulation includes speciated mercury emissions from both natural and anthropogenic sources, as described by Amos et al.[43]. Hg^0 in the atmosphere is oxidized by Br atoms, with Br

concentrations specified by photochemical steady state with a global distribution of BrO concentrations from the p-TOMCAT model. Atmospheric Hg^{II} is partitioned between the gas and aerosol phases, photoreduces to Hg^0 in clouds, and deposits by wet and dry processes[43].

The ocean mixed layer simulation is dynamically coupled to the atmosphere on the 4°x5° grid scale and 1-hour time steps as described by Soerensen et al.[14]. It includes atmospheric input (deposition) of Hg^{II}, exchange of Hg^0 with the atmosphere, exchange with the subsurface waters (see Supplementary Information), partitioning between dissolved and particulate Hg^{II}, and redox Hg^0/Hg^{II} chemistry by photochemical, biological, and thermal processes. Ocean processes are computed in all ocean grid boxes, regardless of sea ice cover, except evasion of Hg^0 to the atmosphere, which occurs only from ocean grid boxes with less than 100% sea ice cover (see Supplementary Information). The ocean model does not include lateral transport. Oceanic and riverine THg concentrations and loads reported here are equivalent to those measured in environmental samples. We assume a fraction of the oceanic (non-Hg^0) THg load is reducible. We do not explicitly simulate methylated mercury speciation (planned for a future version of the model), which will affect species partitioning but will not change the overall pool of THg available for reduction.

Bromine chemistry over polar sea ice. Relative to previous versions of GEOS-Chem[13,14], our simulation includes an improved representation of polar sea ice (from the MERRA assimilated meteorological data archive) and its implications for bromine chemistry. We assume that a polar 4°x5° grid square in GEOS-Chem can generate BrO_x radicals in spring if at least 50% of its native resolution (0.5°x0.667°) grid squares have more than 10% sea ice and if incident

shortwave radiation at the surface is greater than 100 W m^{-2} (ref. 44). Under these conditions and based on the ship and aircraft observations by Pöhler et al.[44] and Prados-Roman et al.[45] in the Arctic in March-April, we specify boundary layer BrO concentrations as a function of MERRA air temperature at 2-m altitude (T) as [BrO] = 20 pptv for $T \leq 248$ K, 10 pptv for $248 < T \leq 253$ K, and 5 pptv for $253 < T \leq 268$ K. Br concentrations are then calculated assuming photochemical steady state, as described by Holmes et al.[13]. The spring time window for BrO_x generation is defined to be February-June in the Arctic and August-December in the Antarctic based on BrO column data from the GOME2 satellite (http://bro.aeronomie.be/level3_monthly.php).

Snowpack photo-reduction and re-emission. Our simulation includes an improved treatment for the fate of Hg^{II} deposited to snow. Photo-reduction of deposited Hg^{II} followed by Hg^0 re-emission is known to take place[19] but not all deposited Hg^{II} is easily reduced[18]. Observational estimates of the reducible component of Hg^{II} range from less than 10%[46] to more than 90%[19]. Here we assume that 60% of deposited Hg^{II} is reducible as in Holmes et al.[13] but test the sensitivity to this assumption. Previous versions of GEOS-Chem used a temperature-based threshold to determine whether photo-reduction and re-emission occurred[13], but this resulted in spring depletion that was too weak in our simulations. In the present implementation, we assume that Hg^{II} photo-reduction for the reducible component is a first-order process with rate constant $k = 2.5\times10^{-9}R$ s^{-1}, where R is the incident solar radiation at the surface in W m^{-2}. The coefficient was chosen to optimize the simulation of Hg^0 in spring. For R = 100 W m^{-2} it implies $k = 1\times10^{-3}$ h^{-1}, in the mid-range of the large spread of observed estimates ranging from 7×10^{-6} to 0.6 h^{-1} (ref. 18). At snowmelt, the entire accumulated non-reducible pool as well as the remaining reducible

pool are eluted with the meltwater[46] and transferred to the underlying ocean or land. Hg^0 re-emitted from the snowpack following photo-reduction is added to the atmospheric reservoir, where it is available for all standard atmospheric processes (e.g. oxidation, deposition, transport).

References

1 Steffen, A., Schroeder, W., Macdonald, R., Poissant, L. & Konoplev, A. Mercury in the Arctic atmosphere: An analysis of eight years of measurements of GEM at Alert (Canada) and a comparison with observations at Amderma (Russia) and Kuujjuarapik (Canada). *Sci. Total Environ.* **342**, 185-198 (2005).

2 Berg, T., Aspmo, K. & Steinnes, E. Transport of Hg from Atmospheric mercury depletion events to the mainland of Norway and its possible influence on Hg deposition. *Geophys. Res. Lett.* **35**, L09802 (2008).

3 Cole, A. S. & Steffen, A. Trends in long-term gaseous mercury observations in the Arctic and effects of temperature and other atmospheric conditions. *Atmos. Chem. Phys.* **10**, 4661-4672 (2010).

4 Selin, N. E. *et al*. Chemical cycling and deposition of atmospheric mercury: Global constraints from observations. *J. Geophys. Res.* **112**, D02308 (2007).

5 Steffen, A. *et al*. A synthesis of atmospheric mercury depletion event chemistry in the atmosphere and snow. *Atmos. Chem. Phys.* **8**, 1445-1482 (2008).

6 Ariya, P. A. *et al*. The Arctic: a sink for mercury. *Tellus B* **56**, 397-403 (2004).

7 Lindberg, S. E. *et al*. Dynamic oxidation of gaseous mercury in the Arctic troposphere at polar sunrise. *Environ. Sci. Tech.* **36**, 1245--1256 (2002).

8 Hirdman, D. *et al*. Transport of mercury in the Arctic atmosphere: Evidence for a spring-time net sink and summer-time source. *Geophys. Res. Lett.* **36**, L12814 (2009).

9 Kirk, J. L., St. Louis, V. L. & Sharp, M. J. Rapid Reduction and Reemission of Mercury Deposited into Snowpacks during Atmospheric Mercury Depletion Events at Churchill, Manitoba, Canada. *Environ. Sci. Tech.* **40**, 7590-7596 (2006).

10 Aspmo, K. *et al*. Mercury in the atmosphere, snow and melt water ponds in the North Atlantic Ocean during Arctic summer. *Environ. Sci. Tech.* **40**, 4083-4089 (2006).

11 Sommar, J., Andersson, M. E. & Jacobi, H.-W. Circumpolar measurements of speciated mercury, ozone and carbon monoxide in the boundary layer of the Arctic Ocean. *Atmos. Chem. Phys.* **10**, 5031-5045 (2010).

12 Andersson, M., Sommar, J., Gårdfeldt, K. & Lindqvist, O. Enhanced concentrations of dissolved gaseous mercury in the surface waters of the Arctic Ocean. *Mar. Chem.* **110**, 190-194 (2008).

13 Holmes, C. D. *et al*. Global atmospheric model for mercury including oxidation by bromine atoms. *Atmos. Chem. Phys.* **10**, 12037-12057 (2010).

14 Soerensen, A. L. *et al*. An improved global model for air-sea exchange of mercury: high concentrations over the North Atlantic. *Environ. Sci. Tech.* **44**, 8574–8580 (2010).

15 Bullock Jr., O. R. *et al*. The North American Mercury Model Intercomparison Study (NAMMIS): Study description and model-to-model comparisons. *J. Geophys. Res.* **113**, D17310 (2008).

16 Task Force on Hemispheric Transport of Air Pollution. Hemispheric Transport of Air Pollution 2010 Part B: Mercury. (Economic Commission for Europe, Geneva, 2010).

17 Steen, A. *et al*. Natural and anthropogenic atmospheric mercury in the European Arctic: a fractionation study. *Atmos*. *Chem*. *Phys*. **11**, 6273--6284 (2011).

18 Durnford, D. & Dastoor, A. The behavior of mercury in the cryosphere: A review of what we know from observations. *J*. *Geophys*. *Res*. **116**, D06305 (2011).

19 Poulain, A. J. *et al*. Redox transformations of mercury in an Arctic snowpack at springtime. *Atmos*. *Environ*. **38**, 6763-6774 (2004).

20 de Boyer Montégut, C., Madec, G., Fischer, A. S., Lazar, A. & Iudicone, D. Mixed layer depth over the global ocean: An examination of profile data and a profile-based climatology. *J*. *Geophys*. *Res*. **109**, C12003 (2004).

21 Toole, J. M. *et al*. Influences of the ocean surface mixed layer and thermohaline stratification on Arctic Sea ice in the central Canada Basin. *J*. *Geophys*. *Res*. **115**, C10018 (2010).

22 Sunderland, E. M. & Mason, R. P. Human impacts on open ocean mercury concentrations. *Global Biogeochem*. *Cy*. **21**, GB4022 (2007).

23 Kirk, J. L. *et al*. Methylated mercury species in marine waters of the Canadian high and sub Arctic. *Environ*. *Sci*. *Tech*. **42**, 8367-8373 (2008).

24 Poulain, A. J. *et al*. Potential for mercury reduction by microbes in the high arctic. *Appl*. *Environ*. *Microb*. **73**, 2230 (2007).

25 Amyot, M., Gill, G. A. & Morel, F. M. M. Production and loss of dissolved gaseous mercury in coastal seawater. *Environ*. *Sci*. *Tech*. **31**, 3606-3611 (1997).

26 Vörösmarty, C. J., Fekete, B. M., Meybeck, M. & Lammers, R. B. Global system of rivers: Its role in organizing continental land mass and defining land-to-ocean linkages. *Global Biogeochem*. *Cy*. **14**, 599-621 (2000).

27 Dittmar, T. & Kattner, G. The biogeochemistry of the river and shelf ecosystem of the Arctic Ocean: A review. *Mar. Chem.* **83**, 103--120 (2003).

28 Grigal, D. Mercury sequestration in forests and peatlands: a review. *J. Environ. Qual.* **32**, 393-405 (2003).

29 Leitch, D. R. *et al*. The delivery of mercury to the Beaufort Sea of the Arctic Ocean by the Mackenzie River. *Sci. Total Environ.* **373**, 178-195 (2007).

30 Coquery, M., Cossa, D. & Martin, J. The distribution of dissolved and particulate mercury in three Siberian estuaries and adjacent Arctic coastal waters. *Water, Air, Soil Pollut.* **80**, 653-664 (1995).

31 Outridge, P., Macdonald, R., Wang, F., Stern, G. & Dastoor, A. A mass balance inventory of mercury in the Arctic Ocean. *Environ. Chem.* **5**, 89-111 (2008).

32 Shiklomanov, A. I. & Lammers, R. B. Record Russian river discharge in 2007 and the limits of analysis. *Environmental Research Letters* **4**, 045015 (2009).

33 Schuster, P. F. *et al*. Mercury Export from the Yukon River Basin and Potential Response to a Changing Climate. *Environ. Sci. Tech.* **45**, 9262-9267 (2011).

34 Walling, D. & Webb, B. Estimating the discharge of contaminants to coastal waters by rivers: some cautionary comments. *Mar. Pollut. Bull.* **16**, 488-492 (1985).

35 Lantuit, H. & Pollard, W. H. Fifty years of coastal erosion and retrogressive thaw slump activity on Herschel Island, southern Beaufort Sea, Yukon Territory, Canada. *Geomorphology* **95**, 84-102, doi:Doi 10.1016/J.Geomorph.2006.07.040 (2008).

36 Atkinson, D. E. Observed storminess patterns and trends in the circum-Arctic coastal regime. *Geo-Mar Lett* **25**, 98-109, doi:Doi 10.1007/S00367-004-0191-0 (2005).

37 Leitch, D. R. *Mercury distribution in water and permafrost of the lower Mackenzie Basin, their contribution to the mercury contamination in the Beaufort Sea marine ecosystem, and potential effects of climate variation* Master of Science thesis, University of Manitoba, (2006).

38 Rachold, V. *et al*. in *The Organic Carbon Cycle in the Arctic Ocean* (eds R. Stein & R. Macdonald) Ch. 2, 33-55 (Springer-Verlag, 2004).

39 Graydon, J. A., Emmerton, C. A., Lesack, L. F. W. & Kelly, E. N. Mercury in the Mackenzie River delta and estuary: Concentrations and fluxes during open-water conditions. *Sci. Total Environ.* **407**, 2980-2988 (2009).

40 Rydberg, J., Klaminder, J., Rosén, P. & Bindler, R. Climate driven release of carbon and mercury from permafrost mires increases mercury loading to sub-arctic lakes. *Sci. Total Environ.* **408**, 4778–4783 (2010).

41 Turetsky, M. R. *et al*. Wildfires threaten mercury stocks in northern soils. *Geophys. Res. Lett.* **33**, 16403 (2006).

42 Reynolds, R. W., Rayner, N. A., Smith, T. M., Stokes, D. C. & Wang, W. An Improved In Situ and Satellite SST Analysis for Climate. *J. Climate* **15**, 1609-1625 (2002).

43 Amos, H. A. *et al*. Gas-particle partitioning of atmospheric Hg(II) and its effect on global mercury deposition. *Atmos. Chem. Phys.* **12**, 591-603 (2012).

44 Pöhler, D., Vogel, L., Frieß, U. & Platt, U. Observation of halogen species in the Amundsen Gulf, Arctic, by active long-path differential optical absorption spectroscopy. *P. Natl. Acad. Sci. USA* **107**, 6582-6587 (2010).

45 Prados-Roman, C. *et al*. Airborne DOAS limb measurements of tropospheric trace gas profiles: case studies on the profile retrieval of O4 and BrO. *Atmospheric Measurement Techniques* **4**, 1241-1260 (2011).

46 Dommergue, A. *et al*. The fate of mercury species in a sub-arctic snowpack during snowmelt. *Geophys. Res. Lett.* **30**, 1621 (2003).

47 Weiss-Penzias, P., Jaffe, D. A., McClintick, A., Prestbo, E. M. & Landis, M. S. Gaseous elemental mercury in the marine boundary layer: Evidence for rapid removal in anthropogenic pollution. *Environ. Sci. Tech.* **37**, 3755-3763 (2003).

48 Sigler, J. M., Mao, H. & Talbot, R. Gaseous elemental and reactive mercury in Southern New Hampshire. *Atmos. Chem. Phys.* **9**, 1929-1942 (2009).

49 Yatavelli, R. L. N. *et al*. Mercury, PM2.5 and gaseous co-pollutants in the Ohio River Valley region: Preliminary results from the Athens supersite. *Atmos. Environ.* **40**, 6650-6665 (2006).

50 Fekete, B. M., Vörösmarty, C. J. & Grabs, W. Global, composite runoff fields based on observed river discharge and simulated water balances. (University of New Hampshire and Global Runoff Data Centre, 2000).

Correspondence and requests for materials should be addressed to J.A. Fisher.

Acknowledgments. This work was funded by the Arctic System Science Program of the U.S. National Science Foundation. Funding support for the Alert and Amderma data sets was provided by the Northern Contaminants Program, Environment Canada, and the Arctic Monitoring and Assessment Programme. We thank Amanda Cole for providing the Alert data; Alexei Konoplev and Fidel Pankratov at SPA Typhoon in Obninsk, Russia for providing the

Amderma data; Katrine Aspmo Pfaffhuber, Torunn Berg, and the Chemical Co-ordinating Centre of EMEP for providing the Zeppelin data; and Elizabeth Corbitt and Christopher Holmes for helpful conversations.

Author Contributions

J.A.F. designed, performed, and interpreted the model simulations. D.J.J. and E.M.S. supervised the research and contributed significantly to interpretation of the results. A.L.S. and H.M.A. developed major components of the model. A.S. collected the Alert data. J.A.F. wrote the paper, and all authors edited and revised the paper.

Competing Financial Interests

The authors declare no competing financial interests.

Tables

Table 1. Comparison between observed and modeled parameters in the Arctic Ocean.

	Reference	**Months**	**Location of observations**	**Observed mean ± standard deviation**	**Modeled mean (70-90°N)**
Ocean [Hg^0]	Andersson et al. (2008)	Jul.-Sep.	Arctic Ocean	0.22 ± 0.11 pM	0.21 pM
Ocean [Hg^0]	Kirk et al. (2008)[a,b]	Aug.-Sep.	Canadian Arctic	0.13 ± 0.05 pM	0.20 pM
Ocean [THg]	Kirk et al. (2008)[a,b]	Aug.-Sep.	Canadian Arctic	2.9 ± 2.9 pM	2.5 pM
Hg^0 evasion flux	Kirk et al. (2008)[a]	Aug.-Sep.	Canadian Arctic	87 ± 102 ng m^{-2} d^{-1}	44 ng m^{-2} d^{-1}
[Hg^0]/[THg]	Kirk et al. (2008)[a]	Aug.-Sep.	Canadian Arctic	7.2 ± 4.9 %	8.2 %
Atmospheric [Hg^0]	Sommar et al. (2010)	Jul.-Sep.	Arctic Ocean	1.72 ± 0.35 ng m^{-3}	1.86 ng m^{-3}
Ocean [Hg^0]	This study[c]	Jun.-Jul.	n/a	--	0.25 pM
Ocean [THg]	This study[c]	Jun.-Jul.	n/a	--	3.0 pM

[a] We include here only the subset of observations from Arctic latitudes north of 68°N (sites 1-11).

[b] Ocean mercury concentrations refer to the surface water concentrations measured by Kirk et al.[23].

[c] Arctic Ocean mercury concentrations have not been measured during early summer (June-July). Modeled values are nonetheless given here to show the seasonal maximum in predicted [Hg^0] and [THg].

Figure Legends

Figure 1 | Seasonal variation of atmospheric elemental mercury (Hg^0). Monthly mean observed Hg^0 concentrations in surface air are shown for the Arctic (solid black line) and U.S. northern mid-latitudes (green line). Arctic values are an average over Alert, Canada (83°N, 62°W; 2005-2009)[1], Zeppelin Mountain, Norway (79°N, 12°E; 2000-2009)[2], and Amderma, Russia (70°N, 62°E; 2001-2003)[1]; individual sites are shown as thin dashed/dotted lines. Values at mid-latitudes are an average over Cheeka Peak, Washington (2001-2002)[47], Pack Monadnock, New Hampshire (2007)[48], Athens, Ohio (2004-2005)[49], and Pensacola, Florida (2005-2008)[13]. The green shading indicates the standard deviation of monthly means among mid-latitude sites.

Figure 2 | Simulated seasonal variation of Hg^0 concentrations in Arctic surface air. Observations (black) are multi-year averages across the three Arctic sites of Fig. 1. Model results are averages over these sites in 2008 for the standard simulation (red) and the sensitivity simulations described in the text: (1) increased reducible percentage of mercury in snow (purple dashed); (2) increased in-snow reduction rate (purple dotted); (3) increased ratio of photo-reduction to photo-oxidation (orange dashed); (4) increased biotic reduction rate (orange dotted); and (5) input of riverine and erosional Hg^{II} to the ocean (blue). The standard deviation among sites is indicated by gray shading for the observations and vertical bars for the simulations.

Figure 3 | Seasonal budget of mercury in the Arctic Ocean mixed layer (70-90°N). Shown are the masses and fluxes of total mercury (THg) in (a) the standard simulation and (b) the optimized simulation including riverine and erosional inputs. The solid black lines show the seasonal variation of THg mass in the ocean mixed layer. Inputs (red and green) include the sources from rivers and erosion, meltwater, subsurface waters via entrainment, and the

atmosphere via Hg^{II} deposition. Outputs (blue) include removal to the atmosphere through net Hg^0 evasion and to the subsurface ocean through detrainment and settling particles.

Figure 4 | Mean seasonal variation of river discharge into the Arctic Ocean. Water discharge is summed over the eight largest circumpolar rivers (solid line) including the Yenisei, Lena, Ob, Pechora, Dvina, and Kolyma in Russia and the Mackenzie and Yukon in North America. The dashed line shows the contribution from Russian rivers only. Discharge data are from the University of New Hampshire Global Runoff Data Centre (UNH-GRDC) Composite Runoff Fields V1.0 (http://www.grdc.sr.unh.edu/index.html), compiled based on long-term monitoring at river gauging stations dating from at least the late 1970s to the mid-1990s (ref. 50).

Figure 5 | Budget of mercury in the high Arctic. Annual budget of mercury for the Arctic surface ocean-atmosphere-cryosphere system (70-90°N) as simulated by GEOS-Chem including the source from circumpolar rivers and coastal erosion. Red arrows show net inputs to the ocean mixed layer, blue arrows show net removal from the ocean mixed layer, gray arrows show atmosphere-cryosphere fluxes, black arrows show partitioning between species, and the green arrow shows net atmospheric export to mid-latitudes. Also shown are modeled Hg^0 and THg concentrations for the ocean. Deposition to ice-free land (<1 Mg a^{-1}) is not shown.

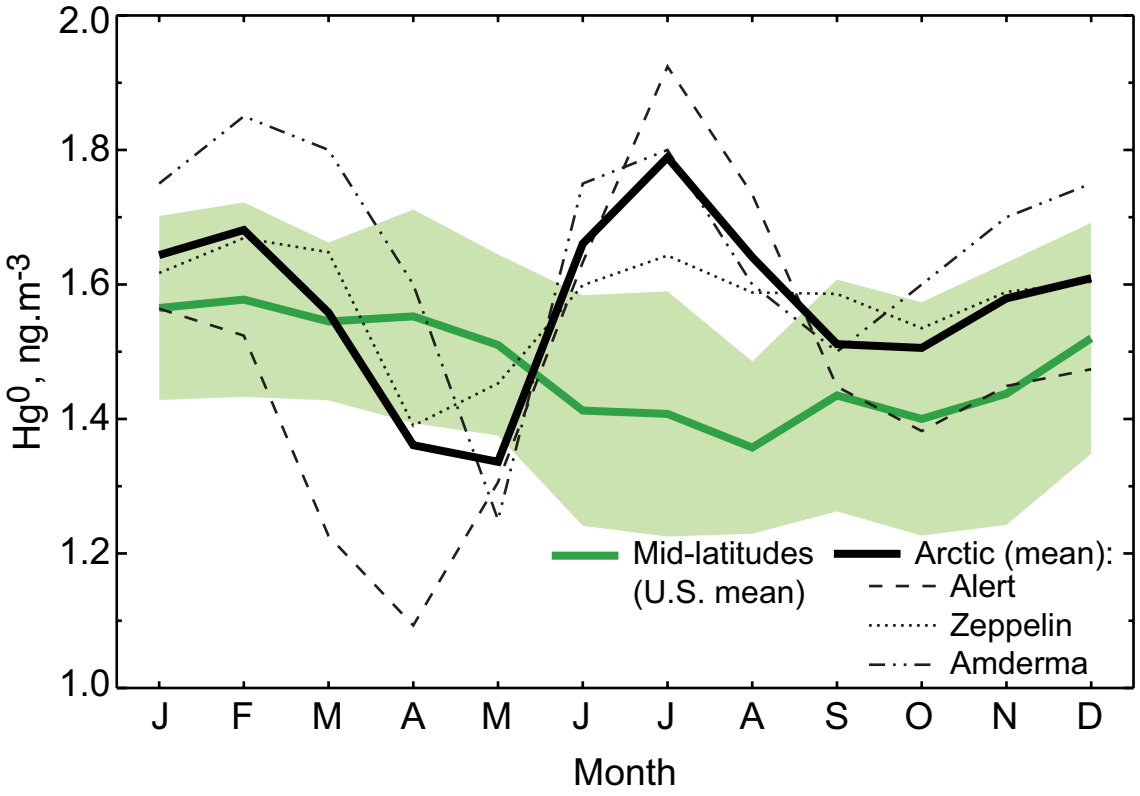
2.0
1.8
1.6
1.4
1.2
1.0
Hg0, ng.m-3
J
F
M
A
M
J
J
A
S
O
N
D
Month
Mid-latitudes
(U.S. mean)
Arctic (mean):
Alert
Zeppelin
Amderma

Figure 1.

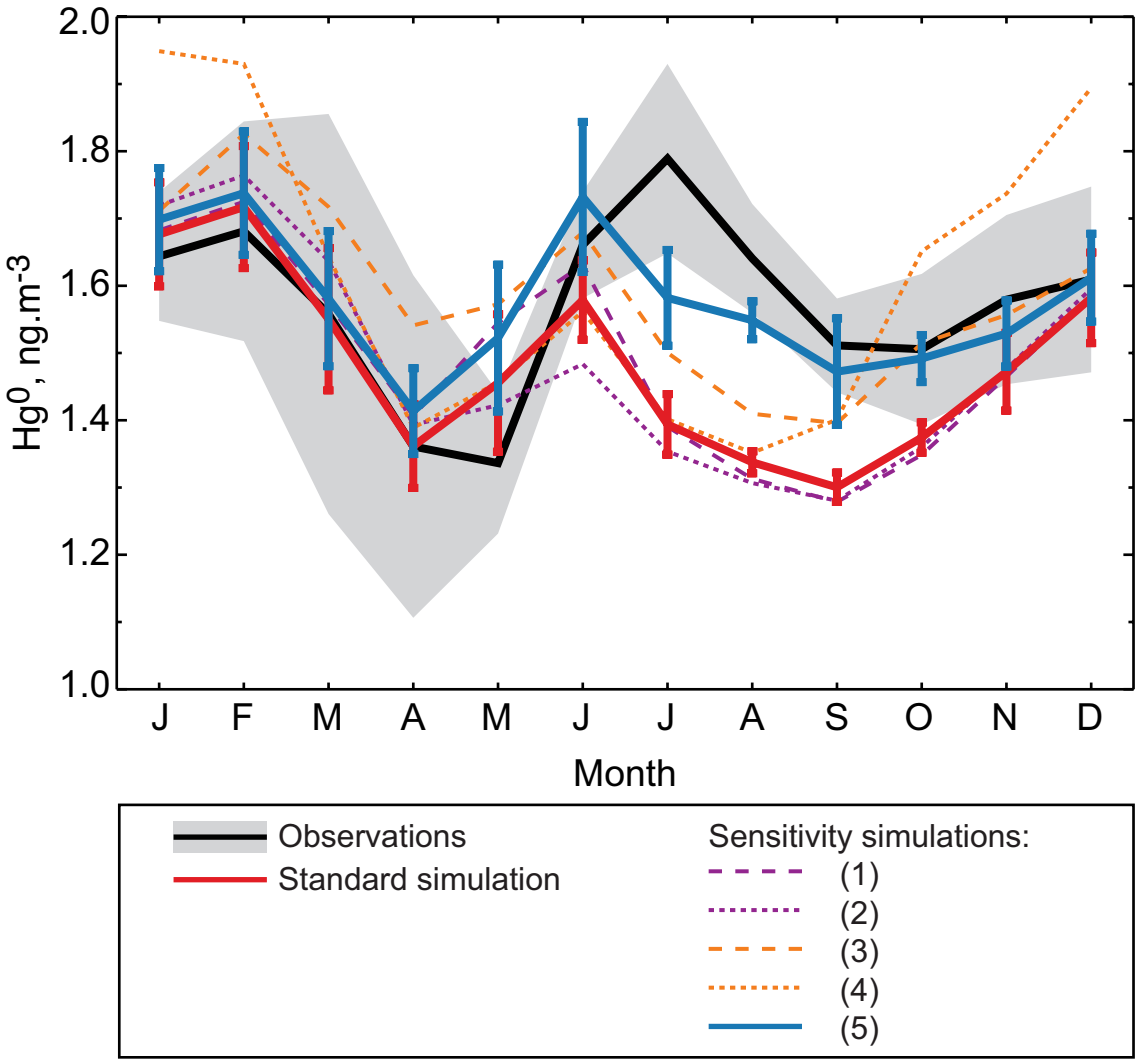
2.0
1.8
1.6
1.4
1.2
1.0
Hg0, ng.m-3
J
F
M
A
M
J
J
A
S
O
N
D
Month
Observations
Standard simulation
Sensitivity simulations:
(1)
(2)
(3)
(4)
(5)

Figure 2.

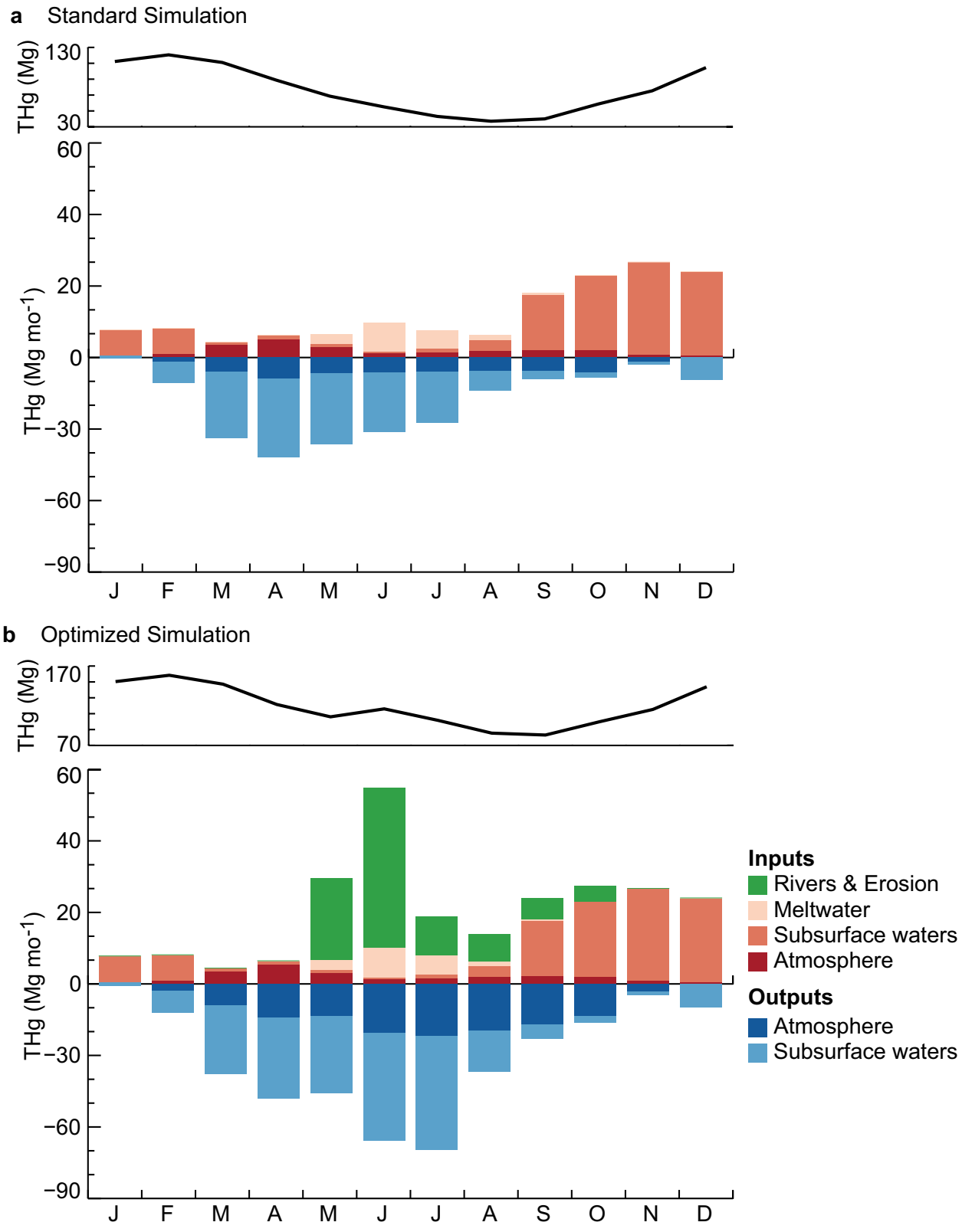
a Standard Simulation
THg (Mg)
130
30
60
40
20
0
−30
−60
−90
THg (Mg mo-1)
J F M A M J J A S O N D
b Optimized Simulation
THg (Mg)
170
70
60
40
20
0
−30
−60
−90
THg (Mg mo-1)
J F M A M J J A S O N D
Inputs
Rivers & Erosion
Meltwater
Subsurface waters
Atmosphere
Outputs
Atmosphere
Subsurface waters

Figure 3.

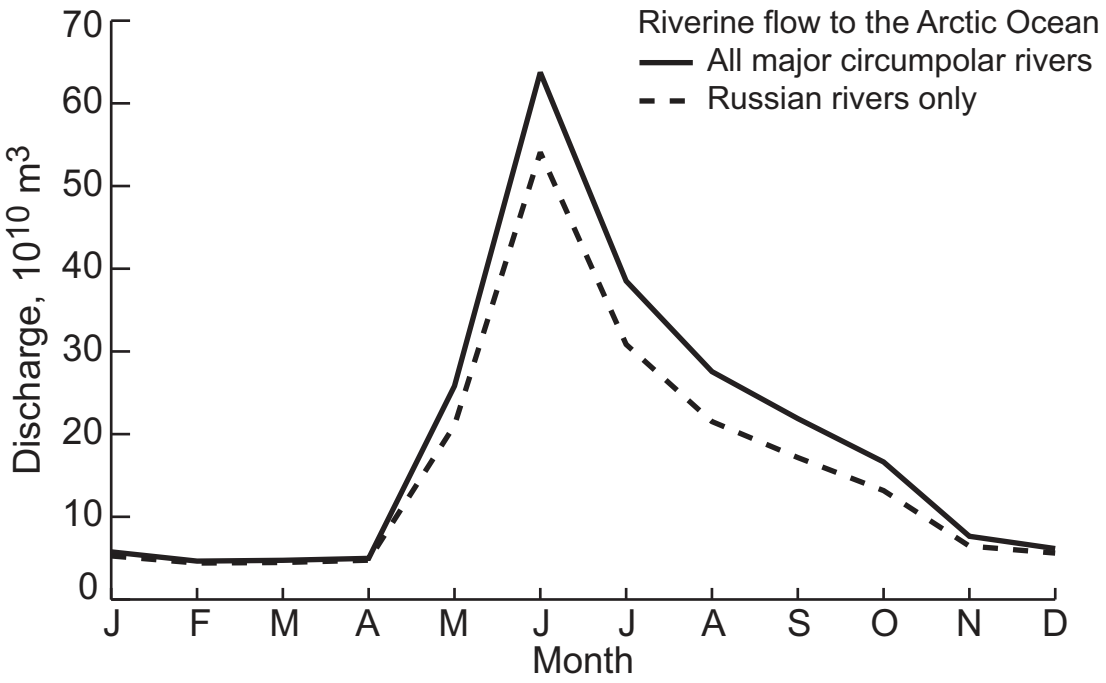
Riverine flow to the Arctic Ocean
All major circumpolar rivers
Russian rivers only
Discharge, 10^{10} m^3
70
60
50
40
30
20
10
0
J
F
M
A
M
J
J
A
S
O
N
D
Month

Figure 4.

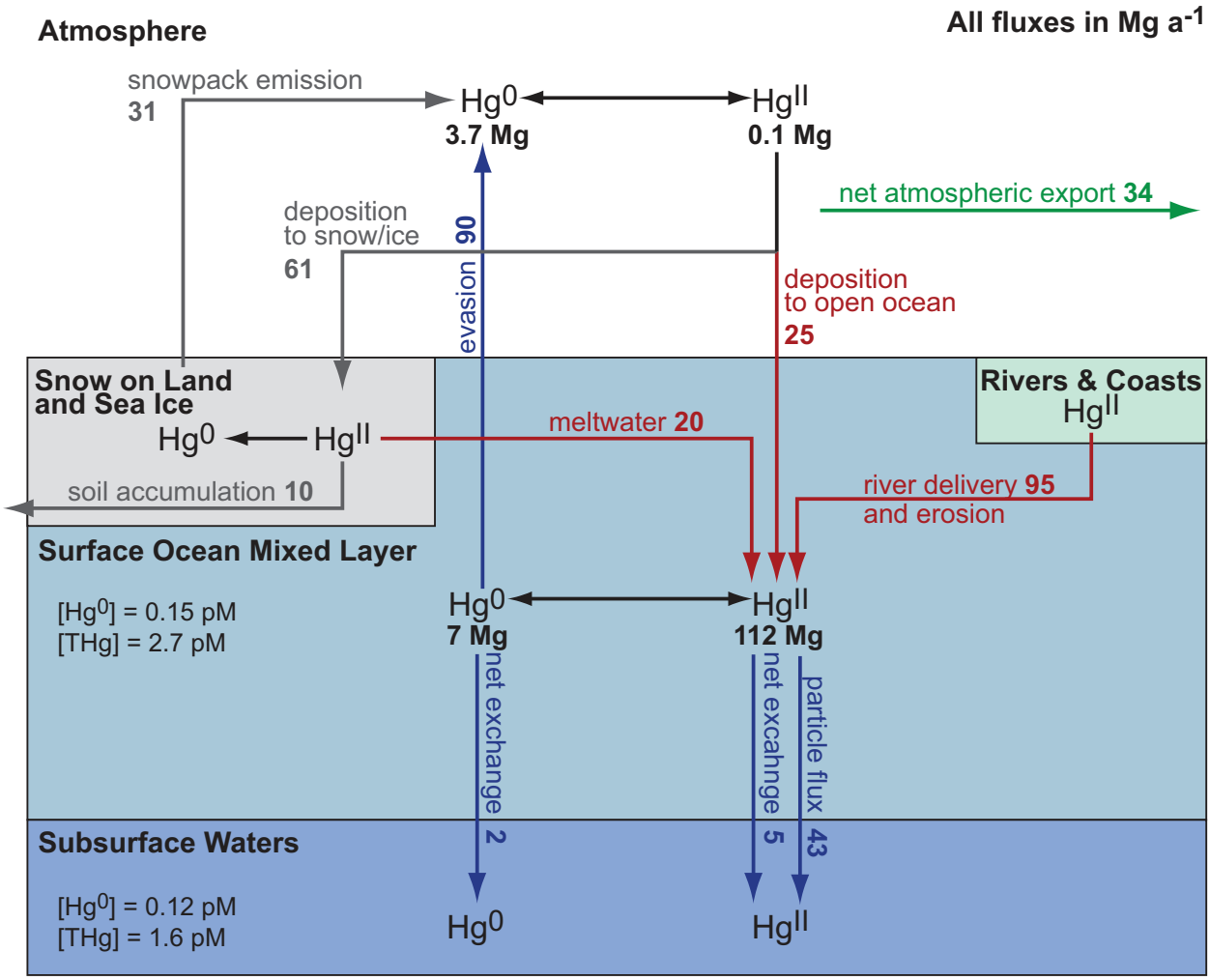
Atmosphere
All fluxes in Mg a-1
snowpack emission
31
Hg0
3.7 Mg
HgII
0.1 Mg
net atmospheric export 34
deposition
to snow/ice
61
90
evasion
deposition
to open ocean
25
Snow on Land
and Sea Ice
Hg0
HgII
meltwater 20
soil accumulation 10
Rivers & Coasts
HgII
river delivery 95
and erosion
Surface Ocean Mixed Layer
[Hg0] = 0.15 pM
[THg] = 2.7 pM
Hg0
7 Mg
HgII
112 Mg
net exchange 2
net exchange 5
particle flux 43
Subsurface Waters
[Hg0] = 0.12 pM
[THg] = 1.6 pM
Hg0
HgII

Figure 5.

Supplementary Information

Major riverine source of Arctic Ocean mercury inferred from atmospheric observations

Jenny A. Fisher[1*], Daniel J. Jacob[1,2], Anne L. Soerensen[2,3], Helen M. Amos[1], Alexandra Steffen[4], and Elsie M. Sunderland[2,3]

[1]Department of Earth and Planetary Sciences, Harvard University, Cambridge, Massachusetts 02138, USA

[2]School of Engineering and Applied Sciences, Harvard University, Cambridge, Massachusetts 02138, USA

[3]Department of Environmental Health, Harvard School of Public Health, Harvard University, Boston, Massachusetts 02215, USA

[4]Air Quality Processes Research Section, Environment Canada, Toronto, Ontario M3H 5T4, Canada

*e-mail: jafisher@fas.harvard.edu

This supplement contains:

1. **Supplementary Information: other unlikely sources**
2. **Supplementary Information: representativeness of river concentration observations**
3. **Supplementary Information: sensitivity to evasion parameterization**
4. **Supplementary Information: sensitivity to export parameterization**
5. **Supplementary Information: sensitivity to riverine source location**
6. **Supplementary Figures (2)**
7. **Supplementary References**

Supplementary Information: other unlikely sources

We find using model sensitivity studies that the standard model is missing a large seasonal source of mercury to the Arctic Ocean mixed layer in spring-summer to counteract the seasonal losses to the subsurface ocean. As we show, this spring-summer source cannot be explained by meltwater delivery or atmospheric deposition. A few unlikely possibilities for this source not discussed in the main text are addressed here.

We find in the model that while most of the mercury in meltwater is transferred to the ocean, a third is transferred to soil, where the model does not track its fate. It seems unlikely that the mercury deposited to soil could be re-emitted quickly enough to explain the summer peak because of the time required for organic matter degradation and release[1]. Note that some of the mercury in soil may be transferred to the ocean through river runoff, a fate we discuss in detail in the text.

An additional possible but unlikely source is transport from the North Atlantic. Penetration of Atlantic water to the Arctic takes place mainly at intermediate depths[2] and would therefore have little impact on the ocean mixed layer in spring-summer due to seasonal stratification from surface heating and freshening. Some North Atlantic inflow does occur at the surface[2] but is minimum in summer[3].

Finally, mercury diffusion from shelf sediments is unlikely to explain the missing source given that large seasonal variations are unexpected and that observed diffusive fluxes are generally <60

pmol m^{-2} d^{-1} (ref. 4), amounting to <22 Mg a^{-1} of THg when applied to the entire Arctic shelf region.

Supplementary Information: representativeness of river concentration observations

Estimating river contaminant loads using concentrations based on a small number of infrequent samples has been shown to lead to large errors[5]. Contaminant transport is dominated by flood events, which are highly episodic. As a result, river measurements generally miss most of the major contaminant transport events. Unless intensive sampling occurs during flood events, loads calculated from mean concentration measurements underestimate real loads. On the River Exe, for example, Walling and Webb[5] use hourly samples to show that 60% of the load is transported during only 2% of the time. They show that computing a mean annual load based on weekly concentration measurements underestimates the true load by 62%, while using monthly measurements underestimates the load by 75%. Similar results have been shown for other rivers[6-9] and demonstrated theoretically[10].

The underestimates are likely to be especially severe for the Russian rivers, where previous flux estimates are based not on weekly or monthly sampling but on a single set of samples from each river. Because these samples were collected in September, several months after peak flow, assuming these numbers represent annual mean concentrations, as done by Outridge et al.[11] will greatly underestimate total river inputs. Increasing these concentration estimates by a factor of three during spring flow, as done by Coquery et al.[12], will account for mean seasonal changes but will still miss the large export during episodic flood events. We therefore expect that previous mercury flux estimates computed in this fashion are significantly lower than true river loads.

Riverine mercury fluxes can also be estimated based on the mass ratio of mercury to organic carbon ($Hg:C_{org}$). However, this ratio is highly uncertain for Arctic rivers, with observations showing values as low as $0.1 \bullet 10^{-6}$ g g^{-1} for the dissolved phase in pristine, sub-Arctic Canadian rivers[13] and as high as $18 \bullet 10^{-6}$ g g^{-1} for particles in the Lena River in Russia[12]. Assuming a total organic carbon flux from rivers to the Arctic Ocean of 30 Tg a^{-1} (ref. 14), these $Hg:C_{org}$ ratios suggest that the THg flux from rivers may be anywhere between 3-540 Mg a^{-1}, illustrating that the loads calculated here are within plausible ranges.

Supplementary Information: sensitivity to evasion parameterization

In the modeled surface ocean, evasion of Hg^0 to the atmosphere is computed for ocean grid boxes with less than 100% sea ice cover. In these boxes, we assume mercury concentrations equilibrate rapidly, and therefore the evasion flux is based on the entire pool of mercury above and below the ice. Because the model does not include lateral transport either within or between ocean grid boxes, this assumption is necessary to prevent non-physical accumulation of mercury under sea ice over long timescales (months to years). Our computed evasion fluxes therefore represent an upper limit. However, model sea ice fractions are likely too high as they are derived from satellite observations. Due to the resolution of the satellite instruments, satellites are known to overestimate sea ice concentration, reporting 100% sea ice cover when surface observations show persistent leads[15]. Small breaks in the ice will not be captured by the model sea ice fractions, and therefore evasion is only computed for grid boxes with sea ice leads that are large enough and persistent enough to be captured by the satellites.

We tested the influence of our evasion assumptions using a sensitivity simulation with the evasion flux from each ocean grid box scaled by the fraction of open water in the grid box, representing a lower limit. This test was performed for both the standard simulation and for the simulation with maximized biotic reduction (4) in order to simulate seasonal under-ice build-up of biologically-produced Hg^0. Results from both sensitivity simulations (shown in Supplementary Fig. 1) show no influence on the ability to simulate the summer peak. This reflects the fact that without an added source, the seasonal cycle of ocean mercury is driven by the losses to the subsurface waters irrespective of the ocean chemistry and evasion fluxes, as described in the main text.

Supplementary Information: sensitivity to export parameterization

Modeled mercury exchange with subsurface waters below the mixed layer depth (MLD) occurs through two processes: seasonal entrainment/detrainment and settling of biological particles. We use a single, seasonally-varying value for MLD across the central Arctic (80-90°N in the Norwegian/Greenland/Barents Seas; 70-90°N elsewhere) based on five years of profile data from Toole et al.[16]. Elsewhere, including in the Norwegian, Greenland, and Barents Seas, a gridded interpolated MLD climatology with monthly resolution is used[17]. MLD in the central Arctic Ocean basin varies from 15 m in summer to 20 m the rest of the year[16]. In the North Atlantic Deep Water formation zone (Norwegian/Greenland/Barents Seas), MLD varies from less than 50 m in summer to more than 300 m in winter[17].

Because the entrainment/detrainment fluxes are physically constrained[17,18], uncertainty in this part of the exchange parameterization comes primarily from the concentration of mercury in the

subsurface waters. Mercury concentrations in subsurface Arctic waters are [THg] = 1.6 pM, specified from observations[19]. Increasing this value in the Arctic Ocean to [THg] = 2.0 pM had no impact on our simulation of atmospheric mercury. In the Arctic as well other oceans, particle settling accounts for the majority of the vertical flux from the ocean mixed layer to the subsurface waters. This flux depends on the coefficient for the partitioning of Hg^{II} between the dissolved and particulate phases (K_D) and the concentration of suspended particulate matter (C_{SPM}), as described for example by Soerensen et al.[18]. For partitioning in the Arctic, we use $\log_{10} K_D = 5.0$ based on measurements from the North Atlantic[20], which provides a better simulation than use of the global value, $\log_{10} K_D = 5.5$. In the model, C_{SPM} is derived from biomass concentrations. In regions of the Arctic where rivers provide additional abiotic particulate matter, C_{SPM} and therefore Hg^{II} settling fluxes may be underestimated. Sensitivity simulations changing C_{SPM} by an order of magnitude resulted in only a 2% change in atmospheric Hg^0 and thus have no influence on simulation of the summer peak.

Supplementary Information: sensitivity to riverine source location

The current implementation of the GEOS-Chem mercury model does not include lateral transport in the surface ocean. As a result, we simulate the river inputs by distributing riverine Hg^{II} uniformly across the Arctic Ocean. This assumption has little impact on simulated atmospheric concentrations because the Arctic atmosphere is well-mixed[21]. For example, previous source attribution studies for mercury[22] and for other species[23,24] have shown that concentrations measured across the Arctic boundary layer derive from a mix of sources, representing mixed background air. To verify that our results were not strongly influenced by the distribution of the riverine mercury source, we performed a sensitivity simulation with riverine Hg^{II} distributed

instead over ocean grid boxes along the Russian coast typically influenced by riverine inputs[25]. We use the same mass of riverine Hg^{II} in both simulations. The results are compared to the original river simulation in Supplementary Fig. 2. The location of the riverine inputs has negligible impact on the summer concentrations of atmospheric Hg^0 averaged over Arctic sites (Fig. S2a). There are small differences between simulations in the geographical distribution of elevated atmospheric Hg^0 in June, but both simulations show large Arctic-wide increases relative to the standard simulation with no river inputs (Fig. S2b).

Supplementary Figures

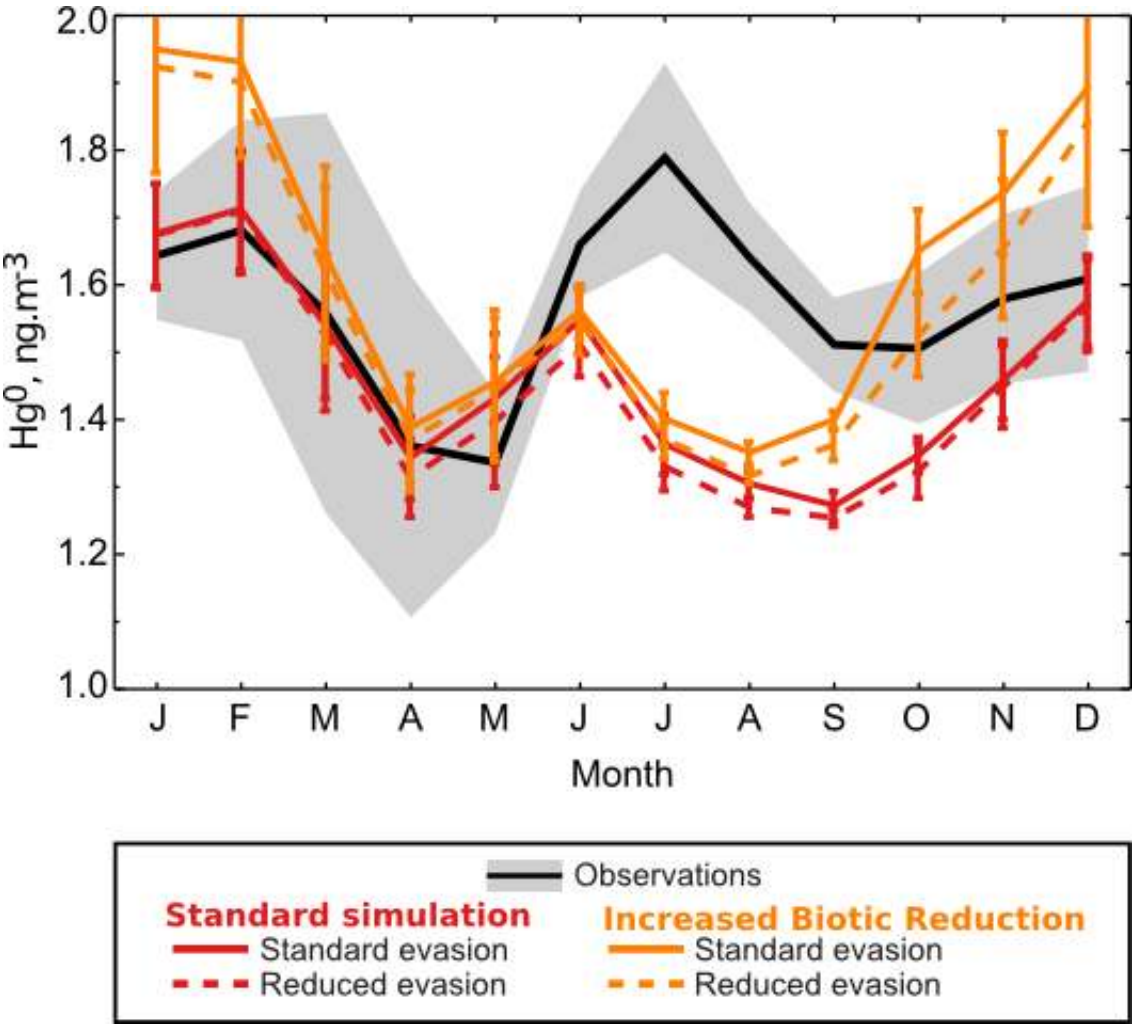

Supplementary Figure 1 | Sensitivity of simulated atmospheric Hg^0 in surface air to evasion parameterization. Mean seasonal cycle at Arctic surface sites from observations (black) and from the standard simulation (red) and the simulation with increased biotic reduction (orange, sensitivity simulation 4 in the main text). Results are shown from each simulation with standard evasion (solid lines) and with evasion scaled to the open water area of each grid box (dashed lines).

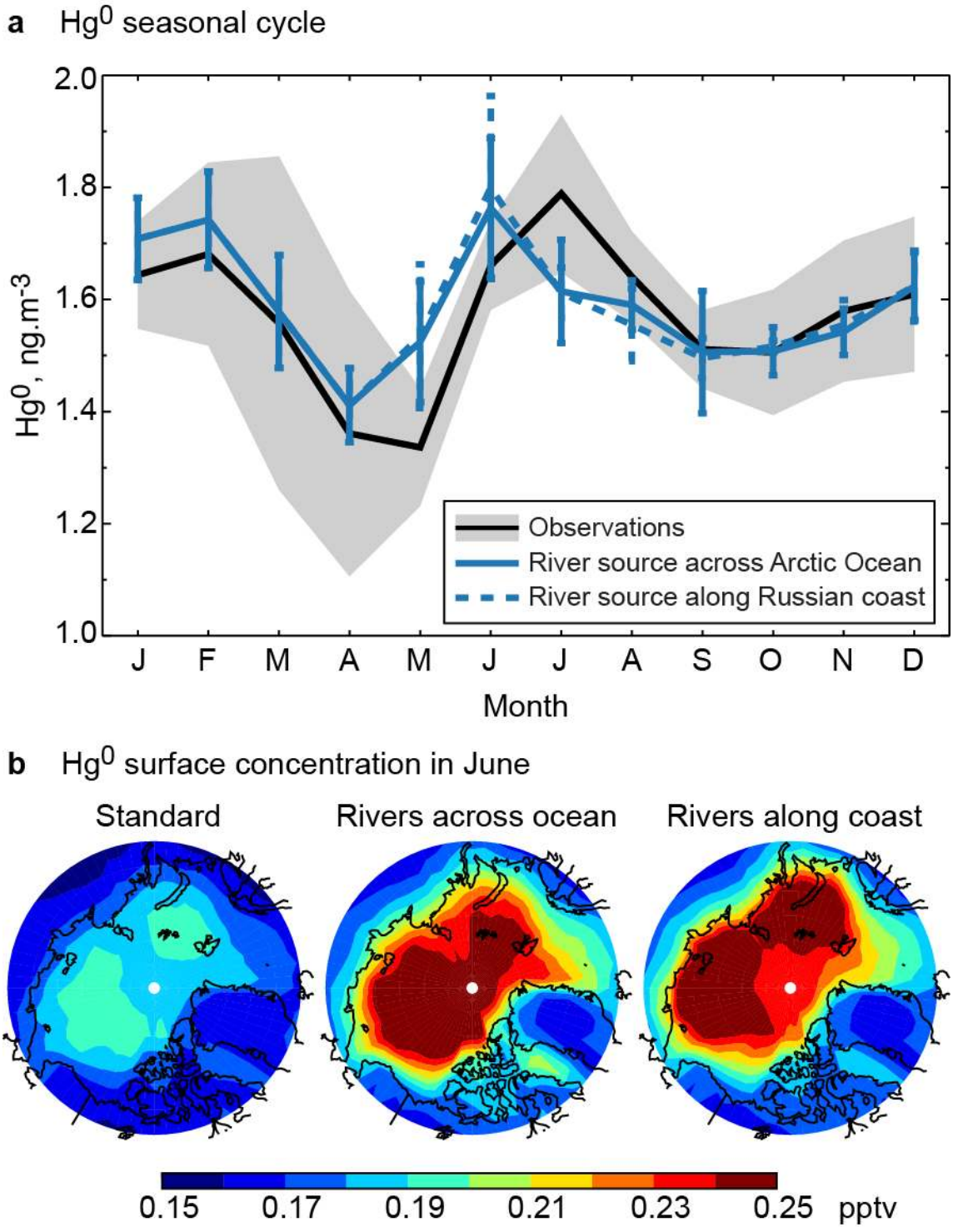

Supplementary Figure 2 | Sensitivity of simulated atmospheric Hg^0 in surface air to location of river input. (a) Mean seasonal cycle at Arctic surface sites from observations (black), the model with riverine Hg^{II} distributed across the Arctic Ocean (blue solid), and the

model with the same total mass of riverine Hg^{II} distributed along the Russian coast (blue dashed). (b) Mean atmospheric surface [Hg^0] in June for the standard model (left), the model with riverine Hg^{II} distributed across the Arctic Ocean (middle), and the model with the same total mass of riverine Hg^{II} distributed along the Russian coast (right).

Supplementary References

1 Smith-Downey, N. V., Sunderland, E. M. & Jacob, D. J. Anthropogenic impacts on global storage and emissions of mercury from terrestrial soils: Insights from a new global model. *J. Geophys. Res.* **115** (2010).

2 Carmack, E. C. in *Polar Oceanography Part A: Physical Science* (ed Jr. Smith, W. O.) (Academic Press, 1990).

3 Orvik, K. A., Skagseth, Ø. & Mork, M. Atlantic inflow to the Nordic Seas: current structure and volume fluxes from moored current meters, VM-ADCP and SeaSoar-CTD observations, 1995-1999. *Deep-Sea Res. Pt. I* **48**, 937-957 (2001).

4 Hollweg, T. A., Gilmour, C. C. & Mason, R. P. Mercury and methylmercury cycling in sediments of the mid-Atlantic continental shelf and slope. *Limnol. Oceanogr.* **55**, 2703-2722 (2010).

5 Walling, D. & Webb, B. Estimating the discharge of contaminants to coastal waters by rivers: some cautionary comments. *Mar. Pollut. Bull.* **16**, 488-492 (1985).

6 Webb, B. W. *et al.* Load estimation methodologies for British rivers and their relevance to the LOIS RACS(R) programme. *Sci. Total Environ.* **194**, 379-389 (1997).

7 Cooper, D. M. & Watts, C. D. A comparison of river load estimation techniques: application to dissolved organic carbon. *Environmetrics* **13**, 733-750, doi:Doi 10.1002/Env.525 (2002).

8 Johnes, P. J. Uncertainties in annual riverine phosphorus load estimation: Impact of load estimation methodology, sampling frequency, baseflow index and catchment population density. *J Hydrol* **332**, 241-258, doi:Doi 10.1016/J.Jhydrol.2006.07.006 (2007).

9 Quémerais, B. *et al*. Sources and Fluxes of Mercury in the St. Lawrence River. *Environ. Sci. Tech.* **33**, 840-849 (1999).

10 Clarke, R. T. Bias and Variance of Some Estimators of Suspended Sediment Load. *Hydrolog Sci J* **35**, 253-261 (1990).

11 Outridge, P., Macdonald, R., Wang, F., Stern, G. & Dastoor, A. A mass balance inventory of mercury in the Arctic Ocean. *Environ. Chem.* **5**, 89-111 (2008).

12 Coquery, M., Cossa, D. & Martin, J. The distribution of dissolved and particulate mercury in three Siberian estuaries and adjacent Arctic coastal waters. *Water, Air, Soil Pollut.* **80**, 653-664 (1995).

13 Kirk, J. L. & St. Louis, V. L. Multiyear Total and Methyl Mercury Exports from Two Major Sub-Arctic Rivers Draining into Hudson Bay, Canada. *Environ. Sci. Tech.* **43**, 2254-2261 (2009).

14 Rachold, V. *et al*. in *The Organic Carbon Cycle in the Arctic Ocean* (eds R. Stein & R. Macdonald) Ch. 2, 33-55 (Springer-Verlag, 2004).

15 Kort, E. A. *et al*. Atmospheric observations of Arctic Ocean methane emissions up to 82° north. *Nature Geoscience* (accepted manuscript).

16 Toole, J. M. *et al*. Influences of the ocean surface mixed layer and thermohaline stratification on Arctic Sea ice in the central Canada Basin. *J. Geophys. Res.* **115**, C10018 (2010).

17 de Boyer Montégut, C., Madec, G., Fischer, A. S., Lazar, A. & Iudicone, D. Mixed layer depth over the global ocean: An examination of profile data and a profile-based climatology. *J. Geophys. Res.* **109**, C12003 (2004).

18 Soerensen, A. L. *et al*. An improved global model for air-sea exchange of mercury: high concentrations over the North Atlantic. *Environ. Sci. Tech.* **44**, 8574–8580 (2010).

19 Kirk, J. L. *et al*. Methylated mercury species in marine waters of the Canadian high and sub Arctic. *Environ. Sci. Tech.* **42**, 8367-8373 (2008).

20 Mason, R. P., Rolfhus, K. R. & Fitzgerald, W. F. Mercury in the North Atlantic. *Mar. Chem.* **61**, 37-53 (1998).

21 Barrie, L. A. & Barrie, M. J. Chemical Components of Lower Tropospheric Aerosols in the High Arctic: Six Years of Observations. *Journal of Atmospheric Chemistry* **11**, 211-226 (1990).

22 Durnford, D. A., Dastoor, A., Figueras-Nieto, D. & Ryjkov, A. Long range transport of mercury to the Arctic and across Canada. *Atmos. Chem. Phys.* **10**, 6063-6086 (2010).

23 Fisher, J. A. *et al*. Sources, distribution, and acidity of sulfate-ammonium aerosol in the Arctic in winter-spring. *Atmos. Environ.* **45**, 7301-7318 (2011).

24 Fisher, J. A. *et al*. Source attribution and interannual variability of Arctic pollution in spring constrained by aircraft (ARCTAS, ARCPAC) and satellite (AIRS) observations of carbon monoxide. *Atmos. Chem. Phys.* **10**, 977-996 (2010).

25 Manizza, M. *et al*. A model of the Arctic Ocean carbon cycle. *J Geophys Res-Oceans* **116**, C12020, doi:10.1029/2011jc006998 (2011).